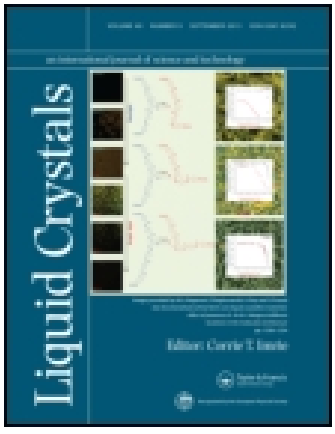

Liquid Crystals

Publication details, including instructions for authors and subscription information:
http://www.tandfonline.com/loi/tlct20

Non-conventional three-armed star-shaped mesogens based on 1,3,5-trisubstituted benzene with azobenzene moieties at the periphery: synthesis, and mesomorphic behaviour

Yew-Hong Ooi[a], Guan-Yeow Yeap[a], Chun-Chieh Han[b], Hong-Cheu Lin[b], Teruo Shinomiya[c] & Masato M. Ito[c]

[a] Liquid Crystal Research Laboratory, School of Chemical Sciences, Universiti Sains Malaysia, Minden, Malaysia

[b] Department of Materials Science and Engineering, National Chiao Tung University, Hsinchu, Taiwan, Republic of China

[c] Department of Environmental Engineering for Symbiosis, Faculty of Engineering, Soka University, Hachioji, Japan

Published online: 17 Mar 2014.

To cite this article: Yew-Hong Ooi, Guan-Yeow Yeap, Chun-Chieh Han, Hong-Cheu Lin, Teruo Shinomiya & Masato M. Ito (2014) Non-conventional three-armed star-shaped mesogens based on 1,3,5-trisubstituted benzene with azobenzene moieties at the periphery: synthesis, and mesomorphic behaviour, Liquid Crystals, 41:7, 1017-1033, DOI: 10.1080/02678292.2014.898341

To link to this article: http://dx.doi.org/10.1080/02678292.2014.898341

Liquid Crystals, 2014
Vol. 41, No. 7, 1017–1033, http://dx.doi.org/10.1080/02678292.2014.898341

Taylor & Francis
Taylor & Francis Group

Non-conventional three-armed star-shaped mesogens based on 1,3,5-trisubstituted benzene with azobenzene moieties at the periphery: synthesis, and mesomorphic behaviour

Yew-Hong Ooi[a], Guan-Yeow Yeap[a]*, Chun-Chieh Han[b], Hong-Cheu Lin[b], Teruo Shinomiya[c] and Masato M. Ito[c]

[a]*Liquid Crystal Research Laboratory, School of Chemical Sciences, Universiti Sains Malaysia, Minden, Malaysia;* [b]*Department of Materials Science and Engineering, National Chiao Tung University, Hsinchu, Taiwan, Republic of China;* [c]*Department of Environmental Engineering for Symbiosis, Faculty of Engineering, Soka University, Hachioji, Japan*

(*Received 8 July 2013; accepted 23 February 2014*)

A series of new symmetrical trimeric star-shaped mesogens in which the molecular architecture composed of three 4-[(4-substituted-phenyl)diazenyl]phenoxy-6-bromohexane connected as the pheripheral units to 1,3,5-positions of the benzene core group have been synthesised and fully characterised by physical measurements and spectroscopic techniques (carbon, hydrogen and nitrogen microanalysis, Fourier transform-infrared spectroscopy and nuclear magnetic resonance: CHN, FT-IR and NMR). At one end of the *para*-position of the azobenzene fragment consists of different terminal substituents X = F, Cl, Br, I, C_2H_5 and OC_2H_5. The thermal behaviour and mesomorphic properties of the star-shaped compounds were investigated by means of differential scanning calorimetry, polarizing optical microscopy (POM) and X-ray diffraction analyses. Moreover, the liquid-crystalline properties of all the intermediates 4-[(4-substituted-phenyl)diazenyl]phenoxy-6-bromohexane were also evaluated. Whilst all the star-shaped compounds exhibit nematic and smectic A phases, the mesogens with chloro- and bromo-terminal substituents were found to show soft crystalline phase. The smectic phase and the possible molecular arrangement of the star-shaped molecule within the anisotropic region were further substantiated by the XRD. In addition to a low-angle sharp peak (reflecting the layered structure), a diffuse wide-angle peak indicating the liquid-like order within the smectic layer was recorded. A comparative study between the properties of the present azo mesogens and the earlier reported star-shaped mesogens from Schiff bases is also discussed.

Keywords: synthesis; star-shaped liquid crystals; azobenzene; terminal substituent; spectroscopic techniques; XRD

1. Introduction

Non-conventional liquid crystals (LCs) have been regarded as new model in the development of LC science and technology as they are capable of exhibiting unique physical properties and unusual phase transition or liquid-crystalline properties which are not common in conventional LCs.[1] The unconventional LCs are generally made up of complex self-organising molecules comprising discrete molecular fragment namely flexible components (alkyl tail or spacer) and several anisometric (mesogenic) segments.[2]

Over the years, there has been a resurgence of interest in the molecular design, synthesis and characterisation of new LCs in which the anisotropic shape is different from that exhibited by the classical rod or disc shapes. Hence, an extensive research and investigation on the non-conventional LCs has been carried out in order to understand the physical and chemical properties of these materials. One of the reasons for researchers to continue working on these LCs can be ascribed to their high potential to self-assemble into a variety of simple-to-complex fluid structures originating either from their parallel alignment or the nano-segregation (either chemically or physically) of the incompatible molecular segments.[2,3]

A number of liquid-crystalline materials with such non-conventional molecular architectures have hitherto been documented in the literature. Some of the typical examples encompass multi-arm mesogens,[4–6] bent-core mesogens,[7–10] dimeric mesogens,[11–14] comb-shaped mesogens [15] and supramolecular mesogens such as metallomesogens [16–18] and hydrogen-bonded mesogens.[19–26] Apart from these, interest in the research of higher non-conventional oligomesogens particularly trimer, tetramer and pentamer has arisen because recent investigations have demonstrated that this class of mesogen possesses the ability to act as model compounds for semi-flexible main chain LC polymers and their unusual transitional properties in comparison with conventional low molar mass LCs.[27]

Star-shaped mesogens or *Hekates* [28] with three extended branches unit connected to a small disc-like core group is considered as one of the simplest non-conventional multi-arm mesogens even though more sophisticated star-shaped LCs containing up to three mesogenic arms have been reported. For instance, the analogous compounds consisted of a discotic

*Corresponding author. Email: gyyeap@usm.my

triphenylene-based core linking with six cyanobiphenyl units via flexible spacer show similar behaviour in which only nematic (N) phase is detected in the liquid-crystalline state.[29,30] Thus, the most commonly used core units in the preparation of the simplest three-armed star-shaped mesogens include benzene ring [31–34] and 1,3,5-triazine group.[35,36] A significant finding on the star-shaped mesogens is that they are found to exhibit diverse optical behaviour consisting of a wide range of phases ranging from crystal, soft crystal, N, smectic, cholesteric to columnar.[31–37] The introduction of various types of mesogenic unit as the peripheral arms connected to a core system can result in significant change upon the liquid-crystalline behaviour due to the combination of two mutually incompatible segments in one molecule. Apart from the nanoscale segregation of incompatible molecular segments, their anisotropic molecular shape and space filling also play a vital role in the self-assembly of mesogens which will result in new mesomorphism.

Azobenzene or simply azo, is often used to refer to a class of molecule with two phenyl rings linked by –N=N– linking group. Azo is known to be a very useful element in synthesising liquid-crystalline materials as they are thermally stable and favourable for mesomorphism.[38–41] Besides, they are also attractive for photo-induced studies as the –N=N– linkage exhibits *trans–cis* isomerisation in the presence of UV light.

We have recently reported a series of star-shaped LCs based on a benzene ring as a central linking group with three Schiff base moieties as peripheral units.[42] They were found to exhibit calamitic mesophases such as N, SmA and SmC. In order to further investigate the liquid-crystalline behaviour and understand the underlying structure–property relationship of 1,3,5-benzene-based star-shaped mesogens, a new series with the azobenzene 4-[(4-substituted-phenyl)diazenyl]phenoxy-6-bromohexane as side-chain units was designed and synthesised. The effect of various terminal substituent, X = F, Cl, Br, I, C_2H_5 and OC_2H_5 of the azobenzene side-chain towards the thermal behaviour of the three-armed star-shaped compounds will be discussed. The liquid-crystalline properties of the intermediary azobenzene fragments were also reported. Since the type of linking group in star-shaped molecules can affect the mesomorphic properties of the respective compounds, therefore, a comparative study between the present series (with N=N linkage) and the earlier reported Schiff base star-shaped analogues (with CH=N linkage) is discussed in this report. Figure 1 shows an illustration of the general molecular structure of the present three-armed star-shaped compounds.

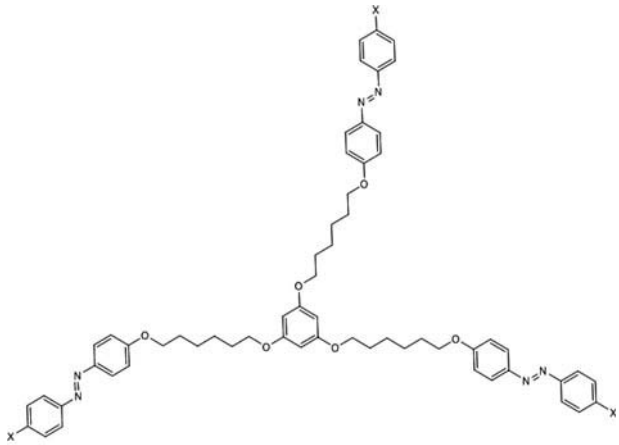

Figure 1. Graphical illustration of the title star-shaped symmetrical mesogens with three azobenzene molecular subunits connected to the central core of benzene group.

2. Experimental

2.1 Reagent and materials

Phloroglucinol anhydrous, 4-fluoroaniline, 4-iodoaniline and 4-ethylaniline were purchased from Acros Organic. 4-Phenetidine was obtained from Sigma-Aldrich while 4-chloroaniline; 4-bromoaniline; 1,6-dibromohexane and phenol were obtained from Merck. Potassium carbonate anhydrous and potassium iodide were purchased from QRec and Fischer Scientific, respectively. Sodium nitrate was obtained from R&M chemicals. All the solvents were used directly from the bottle without further purification.

2.2 Instrumentation and method

The purity and chemical structures of all the intermediates and the final compounds were confirmed by spectroscopic techniques. Fourier transform-infrared spectroscopy (FT-IR) spectra were acquired using a Perkin-Elmer 2000 spectrophotometer (Waltham, MA, USA) where the samples were embedded in KBr pellet and measured in the frequency range of 4000–400 cm^{-1}. ^1H and ^{13}C nuclear magnetic resonance (NMR) spectra were recorded on a 500 MHz Bruker Avance NMR spectrometer (Karlsruhe, Germany). Deuterated chloroform ($CDCl_3$) and dimethylsulphoxide (DMSO-d_6) were used to dissolve the samples along with tetramethylsilane (TMS) as internal standard. In addition, complete atomic assignment of the molecular structure for the star-shaped compounds was further substantiated by means of two-dimensional NMR measurements such as ^1H-^1H COSY, ^1H-^{13}C HMBC and ^1H-^{13}C HMQC. Microanalyses of carbon, hydrogen and nitrogen(CHN) were performed using a Perkin-Elmer

2400 LS (Waltham, MA, USA) series CHNS/O analyser. The UV–Vis spectra were recorded using a Perkin-Elmer Lambda 35 spectrophotometer (Waltham, MA, USA). Optical inspection of the liquid-crystalline phase were determined using a Carls Zeiss polarising optical microscope equipped with a Linkam LTS350 hot stage along with temperature controller. The samples were sandwiched between an ordinary glass slide and a transparent coverslip. Differential scanning calorimetry (DSC) thermograms were recorded on a Seiko DSC120 Model 5500 differential scanning calorimeter by employing a scanning rate of ± 5°C min^{-1} in Soka University, Japan. The enthalpy changes (ΔH) are calculated in kJ mol^{-1} and T is the corresponding phase-transition temperature in degree Celsius (°C).

Synchrotron powder X-ray diffraction (XRD) measurements were performed at beamline BL17A of the National Synchrotron Radiation Research Center, Taiwan, where the wavelength of X-ray was 1.33366 Å. The XRD data were collected using imaging plates (area = 20 × 40 cm^2 with a pixel resolution of 100) curved with a radius equivalent to a sample-to-image plate distance of 280 mm, and the diffraction signals were accumulated for 3 min. The powder samples were packed into capillary tubes heated by a heat gun, whose temperature controller was programmable by a computer with a proportional, integral and differential feedback system. The scattering angle θ was calibrated by a mixture of silver behenate and silicon.

2.3 Synthesis procedures

The star-shaped compounds possess phloroglucinol (1,3,5-trihydroxybenzene) as the central unit. The general synthetic pathway towards the synthesis of azo-based star-shaped compounds is outlined in Scheme 1. Compounds 4-[(4-substituted-phenyl)diazenyl]phenol (**1a–1f**) were prepared through diazonium coupling reaction. Subsequently, alkylation of the intermediary azobenzene with excess of 1,6-dibromohexane was carried out to afford the ω-brominated azobenzene derivatives, **2a–2f**. Finally, phloroglucinol anhydrous was reacted with fourfold excess of compounds **2a–2f** in the presence of potassium carbonate as base and catalytic amount of potassium iodide through Williamson etherification to yield the desired star-shaped mesogens, **3a–3f**.

*2.3.1 Synthesis of 4-[(4-substituted-phenyl)diazenyl] phenol, **1a–1f** (where X = F, Cl, Br, I, C_2H_5 and OC_2H_5)*

Preparation of 4-[(4-substituted-phenyl)diazenyl]phenol was carried out through diazonium coupling reaction between substituted anilines and phenol under cold condition as described in the literature.[43] It is noteworthy to mention that compound **1a** (X = F) has been prepared previously by Attard et al.[44]

*2.3.2 Synthesis of 4-[(4-substituted-phenyl)diazenyl] phenoxy-6-bromohexane, **2a–2f** (where X = F, Cl, Br, I, C_2H_5 and OC_2H_5)*

Azobenzene compounds **1a–1f** (15 mmol) were dissolved in 50 mL acetone in a 100 mL round bottom flask followed by the addition of excess 1,6-dibromohexane (60 mmol) and potassium carbonate anhydrous (45 mmol, 6.2 g) as base. The reaction mixture was then refluxed for overnight before it was allowed to cool down and left to evaporate at room temperature. Cold water was poured into the reaction mixture and the resulting crude precipitate was isolated by suction filtration and rinsed with *n*-hexane in order to remove the excess dibromoalkane. The dried precipitate thus obtained was recrystallised from acetone. The physical results, IR and ^{1}H-NMR along with elemental analysis data for the compounds **2a–2f** were summarised as follows:

2a (X = F): Yield: 62% Brown precipitate. Elemental analysis: found, C 57.34, H 5.40, N 7.34; calculated ($C_{18}H_{20}N_2OBrF$), C 57.00, H 5.32, N 7.39. IR (KBr) ν/cm^{-1}: 2938, 2862 (C–H aliphatic), 1603 (C=C), 1474 (N=N), 1239 (C–O ether). ^{1}H-NMR ($CDCl_3$) δ/ppm: 1.50–1.56 (m, 4H, CH_2), 1.80–1.95 (m, 4H, CH_2), 3.43 (t, 2H, Br–CH_2), 4.04 (t, 2H, O–CH_2), 6.99 (d, 2H, Ar), 7.17 (t, 2H, Ar), 7.86–7.90 (m, 4H, Ar).

2b (X = Cl): Yield: 65% light brown precipitate. Elemental analysis: found, C 54.74, H 4.98, N 7.01; calculated ($C_{18}H_{20}N_2OBrCl$), C 54.63, H 5.09, N 7.08. IR (KBr) ν/cm^{-1}: 2938, 2862 (C–H aliphatic), 1603 (C=C), 1475 (N=N), 1245 (C–O ether). ^{1}H-NMR ($CDCl_3$) δ/ppm: 1.53–1.58 (m, 4H, CH_2), 1.82–1.97 (m, 4H, CH_2), 3.46 (t, 2H, Br-CH_2), 4.07 (t, 2H, O–CH_2), 7.02 (d, 2H, Ar), 7.48 (d, 2H, Ar), 7.84 (d, 2H, Ar), 7.92 (d, 2H, Ar).

2c (X = Br): Yield: 67% brown precipitate. Elemental analysis: found, C 49.31, H 4.59, N 6.46; calculated ($C_{18}H_{20}N_2OBr_2$), C 49.12, H 4.58, N 6.36. IR (KBr) ν/cm^{-1}: 2938, 2862 (C–H aliphatic), 1603 (C=C), 1475 (N=N), 1245 (C–O ether). ^{1}H-NMR ($CDCl_3$) δ/ppm: 1.53–1.58 (m, 4H, CH_2), 1.82–1.98 (m, 4H, CH_2), 3.46 (t, 2H, Br–CH_2), 4.07 (t, 2H, O–CH_2), 7.02 (d, 2H, Ar), 7.64 (d, 2H, Ar), 7.77 (d, 2H, Ar), 7.92 (d, 2H, Ar).

2d (X = I): Yield: 61% Brown precipitate. Elemental analysis: found, C 44.53, H 4.25, N 5.73; calculated ($C_{18}H_{20}N_2OBrI$), C 44.38, H 4.14, N 5.75.

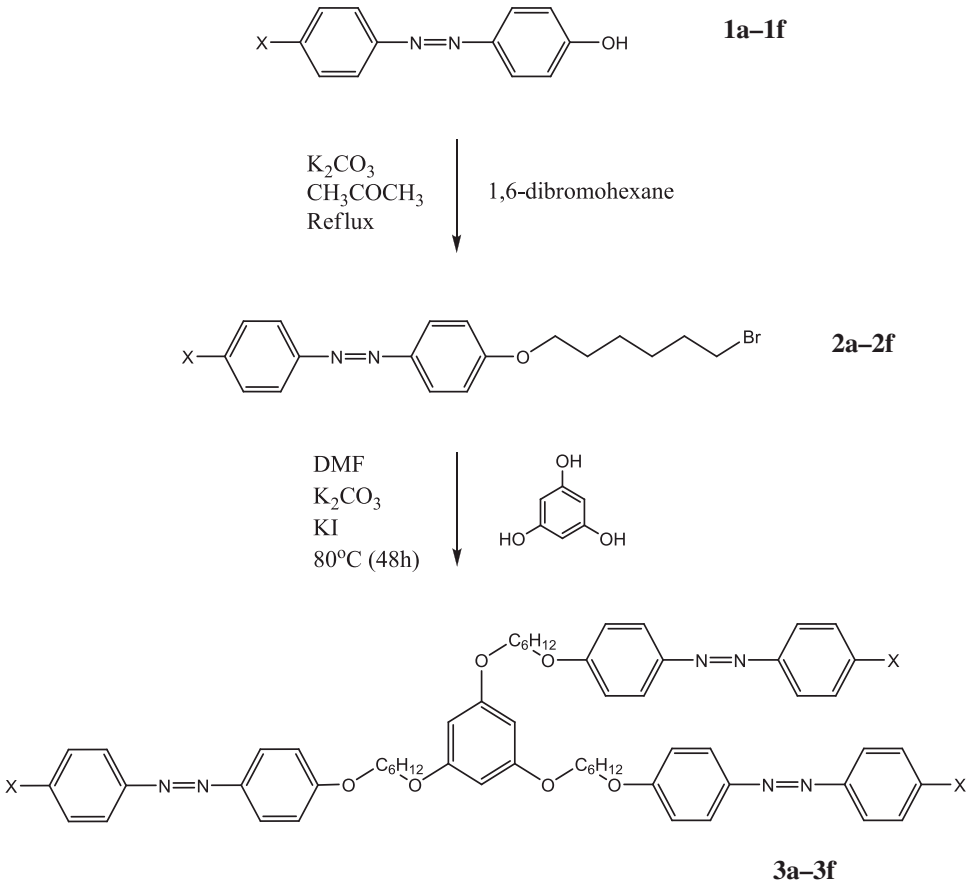

Compound	X
a	F
b	Cl
c	Br
d	I
e	C_2H_5
f	OC_2H_5

Scheme 1. Synthetic route towards the formation of **1a–1f**, **2a–2f**, and the three-armed star-shaped compounds **3a–3f**.

IR (KBr) ν/cm^{-1}: 2940, 2866 (C–H aliphatic), 1605 (C=C), 1477 (N=N), 1248 (C–O ether). ^{1}H-NMR ($CDCl_3$) δ/ppm: 1.49–1.54 (m, 4H, CH_2), 1.80–1.94 (m, 4H, CH_2), 3.42 (t, 2H, Br–CH_2), 4.03 (t, 2H, O–CH_2), 6.97 (d, 2H, Ar), 7.59 (d, 2H, Ar), 7.81 (d, 2H, Ar), 7.88 (d, 2H, Ar).

2e (X = C_2H_5): Yield: 60% Brown precipitate. Elemental analysis: found, C 61.83, H 6.44, N 7.32; calculated ($C_{20}H_{25}N_2OBr$), C 61.70, H 6.47, N 7.20. IR (KBr) ν/cm^{-1}: 2966, 2939, 2863 (C–H aliphatic), 1603 (C=C), 1464 (N=N), 1257 (C–O ether). ^{1}H-NMR ($CDCl_3$) δ/ppm: 1.30 (t, 3H, CH_3), 1.53–1.58 (m, 4H, CH_2), 1.82–1.98 (m, 4H, CH_2), 2.70–2.78 (q, 2H, CH_2), 3.46 (t, 2H, Br–CH_2), 4.06 (t, 2H, O–CH_2), 7.01 (d, 2H, Ar), 7.34 (d, 2H, Ar), 7.83 (d, 2H, Ar), 7.91 (d, 2H, Ar).

2f (X = OC_2H_5): Yield: 58% Brown precipitate. Elemental analysis: found, C 59.55, H 6.29, N 6.88; calculated ($C_{20}H_{25}N_2O_2Br$), C 59.26, H 6.22, N 6.91. IR (KBr) ν/cm^{-1}: 2959, 2938, 2862 (C–H aliphatic), 1602 (C=C), 1474 (N=N), 1247 (C–O ether). ^{1}H-NMR ($CDCl_3$) δ/ppm: 1.48 (t, 3H, CH_3), 1.50–1.58 (m, 4H, CH_2), 1.81–1.96 (m, 4H, CH_2), 3.44 (t, 2H, Br–CH_2), 4.04 (t, 2H, O–CH_2), 4.08–4.15 (q, 2H, OCH_2), 6.98 (d, 4H, Ar), 7.86 (d, 4H, Ar).

*2.3.3 Synthesis of 1,3,5-tris-{4-[(4-substituted-phenyl)diazenyl]phenoxy}-6'-hexyloxy benzene, **3a–3f** (where substituent X = F, Cl, Br, I, C_2H_5 and OC_2H_5)*

In a round bottom flask, phloroglucinol anhydrous (2.0 mmol, 0.25 g) was dissolved in 10 mL of acetone.

Anhydrous potassium carbonate (40 mmol, 4.4 g) was added to the solution and the reaction mixture was heated at reflux for 1 h. Excess amount of compound **2** (8.0 mmol) was dissolved in 50 mL hot *N,N′*-dimethylformamide (DMF) and was subsequently added to the reaction mixture followed by a catalytic amount of potassium iodide. The reaction mixture was heated at 80°C for 48 h. It was then allowed to cool down and left to evaporate at room temperature until the total volume of mixture was 40 mL. Ice water (50 mL) was added and the resulting precipitate was filtered off and dried. The crude precipitate was subjected to column chromatography with chloroform as the mobile phase. The precipitate thus obtained was recrystallised from ethyl acetate to afford the pure star-shaped compounds **3a–3f**. The physical results, IR, ^{1}H- and ^{13}C-NMR along with elemental analysis data for the compounds **3a–3f** were summarised as follows:

3a (X = F): Yield: 36% Brown precipitate. Elemental analysis: found, C 70.73, H 6.35, N 8.25; calculated ($C_{60}H_{63}N_6O_6F_3$), C 70.57, H 6.22, N 8.23. IR (KBr) ν/cm^{-1}: 2941, 2867 (C–H aliphatic), 1602, 1583 (C=C), 1472 (N=N), 1252 (C–O ether). ^{1}H-NMR ($CDCl_3$) δ/ppm: 1.54–1.60 (m, 4H, CH_2), 1.81–1.89 (m, 4H, CH_2), 3.93 (t, 2H, O–CH_2), 4.04 (t, 2H, O–CH_2), 6.08 (s, 1H, Ar), 6.99 (d, 2H, Ar), 7.17 (t, 2H, Ar), 7.86–7.91 (m, 4H, Ar). ^{13}C-NMR ($CDCl_3$) δ/ppm: 164.96 ($C_{aromatic}$–F), 161.68, 160.97 ($C_{aromatic}$–O), 149.32, 146.75 ($C_{aromatic}$–N), 124.70, 124.39, 116.00, 114.75, 93.94 ($C_{aromatic}$), 68.21, 67.84 (C–O), 29.17, 29.13, 25.88, 25.82 ($C_{aliphatic}$).

3b (X = Cl): Yield: 31% Yellow precipitate. Elemental analysis: found, C 67.43, H 5.84, N 7.89; calculated ($C_{60}H_{63}N_6O_6Cl_3$), C 67.32, H 5.93, N 7.85. IR (KBr) ν/cm^{-1}: 2940, 2867 (C–H aliphatic), 1600, 1583 (C=C), 1472 (N=N), 1250 (C–O ether). ^{1}H-NMR ($CDCl_3$) δ/ppm: 1.54–1.60 (m, 4H, CH_2), 1.80–1.88 (m, 4H, CH_2), 3.95 (t, 2H, O–CH_2), 4.06 (t, 2H, O–CH_2), 6.09 (s, 1H, Ar), 7.01 (d, 2H, Ar), 7.47 (d, 2H, Ar), 7.84 (d, 2H, Ar), 7.91 (d, 2H, Ar). ^{13}C-NMR ($CDCl_3$) δ/ppm: 161.90, 160.97 ($C_{aromatic}$–O), 151.18, 146.76 ($C_{aromatic}$–N), 136.10 ($C_{aromatic}$–Cl), 129.24, 124.88, 123.81, 114.78, 93.94 ($C_{aromatic}$), 68.19, 67.84 (C–O), 29.17, 29.12, 25.88, 25.82 ($C_{aliphatic}$).

3c (X = Br): Yield: 32% Yellow precipitate. Elemental analysis: found, C 59.95, H 5.31, N 7.03; calculated ($C_{60}H_{63}N_6O_6Br_3$), C 59.86, H 5.27, N 6.98. IR (KBr) ν/cm^{-1}: 2941, 2868 (C–H aliphatic), 1600, 1583 (C=C), 1473 (N=N), 1247 (C–O ether). ^{1}H-NMR ($CDCl_3$) δ/ppm: 1.51–1.58 (m, 4H, CH_2), 1.79–1.86 (m, 4H, CH_2), 3.93 (t, 2H, O–CH_2), 4.04 (t, 2H, O–CH_2), 6.07 (s, 1H, Ar), 6.99 (d, 2H, Ar), 7.61 (d, 2H, Ar), 7.75 (d, 2H, Ar), 7.89 (d, 2H, Ar). ^{13}C-NMR ($CDCl_3$) δ/ppm: 161.90, 160.92 ($C_{aromatic}$–O), 151.48, 146.70 ($C_{aromatic}$–N), 124.49 ($C_{aromatic}$–Br), 132.22, 124.90, 124.05, 114.75, 93.80 ($C_{aromatic}$), 68.20, 67.79 (C–O), 29.15, 29.10, 25.87, 25.81 ($C_{aliphatic}$).

3d (X = I): Yield: 29% Brown precipitate. Elemental analysis: found, C 53.78, H 4.73, N 6.22; calculated ($C_{60}H_{63}N_6O_6I_3$), C 53.58, H 4.72, N 6.25. IR (KBr) ν/cm^{-1}: 2942, 2870 (C–H aliphatic), 1602, 1585 (C=C), 1476 (N=N), 1250 (C–O ether). ^{1}H-NMR ($CDCl_3$) δ/ppm: 1.50–1.56 (m, 4H, CH_2), 1.77–1.85 (m, 4H, CH_2), 3.90 (t, 2H, O–CH_2), 4.02 (t, 2H, O–CH_2), 6.05 (s, 1H, Ar), 6.96 (d, 2H, Ar), 7.58 (d, 2H, Ar), 7.80 (d, 2H, Ar), 7.87 (d, 2H, Ar). ^{13}C-NMR ($CDCl_3$) δ/ppm: 161.97, 160.96 ($C_{aromatic}$–O), 152.15, 146.75 ($C_{aromatic}$–N), 138.26, 124.95, 124.23, 114.79, 93.90 ($C_{aromatic}$), 96.90 ($C_{aromatic}$–I), 68.24, 67.83 (C–O), 29.17, 29.12, 25.88, 25.82 ($C_{aliphatic}$).

3e (X = C_2H_5): Yield: 36% Brown precipitate. Elemental analysis: found, C 75.68, H 7.54, N 8.03; calculated ($C_{66}H_{78}N_6O_6$), C 75.40, H 7.48, N 7.99. IR (KBr) ν/cm^{-1}: 2965, 2939, 2863 (C–H aliphatic), 1603, 1582 (C=C), 1473 (N=N), 1257 (C–O ether). ^{1}H-NMR ($CDCl_3$) δ/ppm: 1.26 (t, 3H, CH_3), 1.52–1.58 (m, 4H, CH_2), 1.77–1.85 (m, 4H, CH_2), 2.66-2.74 (q, 2H, CH_2), 3.91 (t, 2H, O–CH_2), 4.02 (t, 2H, O–CH_2), 6.06 (s, 1H, Ar), 6.97 (d, 2H, Ar), 7.30 (d, 2H, Ar), 7.79 (d, 2H, Ar), 7.87 (d, 2H, Ar). ^{13}C-NMR ($CDCl_3$) δ/ppm: 161.39, 160.92 ($C_{aromatic}$–O), 151.03, 146.96 ($C_{aromatic}$–N), 147.03, 128.48, 124.56, 122.59, 114.66, 93.80 ($C_{aromatic}$), 68.15, 67.80 (C–O), 29.15, 29.12, 28.79, 25.87, 25.82, ($C_{aliphatic}$), 15.44 (CH_3).

3f (X = OC_2H_5): Yield: 40% Brown precipitate. Elemental analysis: found, C 72.35, H 7.27, N 7.71; calculated ($C_{66}H_{78}N_6O_9$), C 72.11, H 7.15, N 7.64. IR (KBr) ν/cm^{-1}: 2976, 2938, 2868 (C–H aliphatic), 1600, 1581 (C=C), 1474 (N=N), 1243 (C–O ether). ^{1}H-NMR ($CDCl_3$) δ/ppm: 1.47 (t, 3H, CH_3), 1.52–1.58 (m, 4H, CH_2), 1.78–1.86 (m, 4H, CH_2), 3.95 (t, 2H, O–CH_2), 4.05–4.16 (m, 4H, O–CH_2), 6.09 (s, 1H, Ar), 7.00 (d, 4H, Ar), 7.88 (d, 4H, Ar). ^{13}C–NMR ($CDCl_3$) δ/ppm: 161.12, 160.99, 160.95 ($C_{aromatic}$–O), 146.99 ($C_{aromatic}$–N), 124.32, 114.66, 114.67, 93.86 ($C_{aromatic}$), 68.15, 67.83, 63.78 (C–O), 29.17, 29.15, 25.89 25.84 ($C_{aliphatic}$), 14.79 (CH_3).

3. Result and discussions

3.1 Thermal stability and liquid-crystalline properties

The phase transition temperatures and associated enthalpies for the substituted bromohexyloxyazobenzenes **2a–2f** as inferred from the DSC experiments are summarised in Table 1. Although compound **2a** has

been prepared previously by Attard et al. but the calorimetric study is not described,[44] hence the thermal properties for **2d** will be presented herein. From the DSC, it is clear that compounds **2a** and **2d** exhibit crystal–isotropic transition on heating and cooling cycles. Hence, they can be classified as non-mesogens. However, compounds **2b** and **2c** with respective chloro and bromo substituent at terminal position exhibit monotropic (metastable) behaviour. When viewed under polarising microscope, **2b** exhibits a monotropic N phase with a typical marble and thread-like texture as shown in Figure 2a. On further cooling, the appearance of smectic A (SmA) phase is observed and is recognised by the formation of fan-shaped texture. As for **2c** only the fan-shaped of SmA phase in their liquid-crystalline state (Figure 2b) is observed.

As for **2e**, no mesophase is observed on heating. However, on cooling from the isotropic, the N phase is apparent and accompanied by immediate crystallisation as depicted in Figure 2d. It is noteworthy to mention that the exotherm involving the isotropic–N transition could not be detected in the DSC thermogram of **2e**, instead only one endotherm (on heating) and one exotherm (on cooling) associated with the crystal–isotropic transition is observed. The polarizing optical microscopy (POM) observation shows that the mesophase is absent when a rate of 10°C/min is employed as **2e** undergoes direct crystallisation. In other words, the N phase range for **2e** is too narrow and the formation of N phase can only be observed by employing lower cooling rate of 2°C/min. When the terminal substituent is replaced by an ethoxy group ($-OC_2H_5$), the N–isotropic transition temperature as well as the mesophase stability for compound **2f** become higher than those in compound **2e**. This phenomenon can be rationalised in term of the presence of an electronegative oxygen atom in the ethoxy group which enhances the polarisability apart from extending the length of the rigid azobenzene aromatic core.[45] Although the difference between **2e** and **2f** only due to the presence of an oxygen atom, but **2e** is found to be monotropic while **2f** exhibits enanatiotropic behaviour. The N phase is assigned from the

Table 1. Phase transition temperature (°C) and associated enthalpy changes (kJ mol^{-1}) for azobenzene intermediates **2a–2f** upon heating and cooling.

Compound	Phase transition temperatures, °C (ΔH, kJ mol^{-1})
2a (X = F)	Cr 78.8 (46.3) I
	I 67.7 (48.2) Cr
2b (X = Cl)	Cr 83.4 (45.1) I
	I 74.6 (2.0) N 66.2 (16.1) SmA 63.5 (24.2) Cr
2c (X = Br)	Cr 99.3 (42.8) I
	I 77.5 (19.5) SmA 54.7 (9.6) Cr
2d (X = I)	Cr 110.8 (45.0) I
	I 96.6 (9.0) Cr_1 77.2 (27.6) Cr_2
2e (X = C_2H_5)	Cr 87.3 (45.2) I
	I 70.6 (40.9) N & Cr
2f (X = OC_2H_5)	Cr 98.2 (45.8) N 122.3 (1.0) I
	I 121.2 (1.1) N 91.4 (42.6) Cr

Notes: Cr, Crystal; SmC, smectic C; SmA, smectic A; N, nematic; I, isotropic.
*Phase sequence and temperature upon cooling are shown in *italic*.

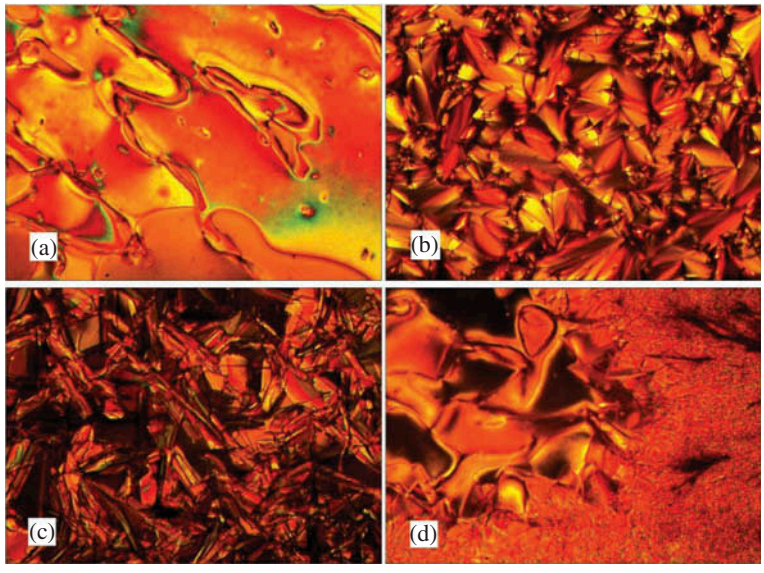

Figure 2. (colour online) Optical photomicrograph of (a) intermediate **2b** (X = Cl) exhibiting the marble texture of nematic phase. (b) Intermediate **2c** (X = Br) exhibiting the fan-shaped texture of SmA phase. (c) Intermediate **2d** (X = I) exhibiting the crystal phase and (d) intermediate **2e** (X = C_2H_5) exhibiting the nematic phase followed by immediate crystallisation.

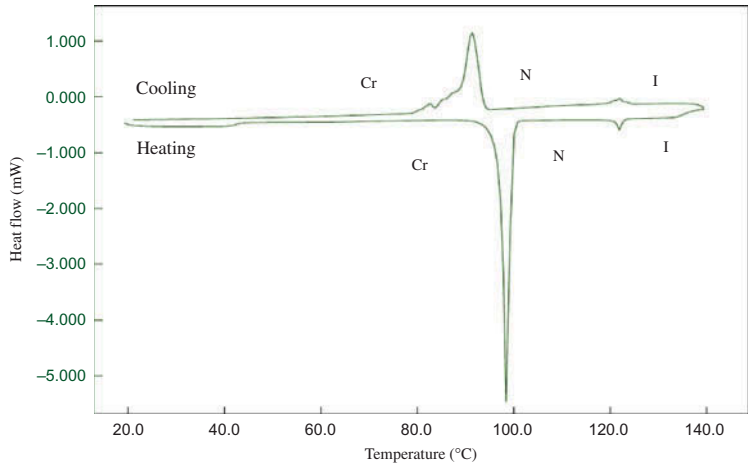

Figure 3. (colour online) DSC thermograms of intermediate **2f** (X = OC_2H_5) upon heating–cooling cycle at the rate of ±5°C.

Schlieran texture containing both types of singularity which flashed when subjected to mechanical stress. The DSC thermograms upon heating–cooling for the representative compounds **2f** (X = OC_2H_5) are depicted in Figure 3.

The phase sequences, transition temperatures and the enthalpy values for the star-shaped mesogens **3a–3f** are summarised in Table 2. All the trimeric star-shaped mesogens exhibit liquid-crystalline behaviour. From the DSC and POM results, compounds **3a** and **3e** show monotropic properties while **3b**, **3c**, **3d** and **3f** appear to be enantiotropic in nature. Compound **3a** (X = F) undergoes melting from crystal to isotropic state when the sample is heated to 110.2°C. Subsequently, on cooling the formation of focal conic fan-shaped texture of SmA phase is observed followed by crystallisation at 73.7°C. Hence, the fluoro-substituted star-shaped mesogen is solely smectogenic. Compound **3b** (*X* = Cl) shows both N and SmA phases. Upon cooling the N phase is apparent with the appearance of Schlieran texture before changing into the focal conic fan-shaped texture of SmA phase. Interestingly, **3b** does not undergo direct crystallisation at lower temperature. In fact, the anisotropic liquid eventually transforms into a soft crystal B phase due to the small enthalpy change as inferred from the DSC thermogram. The soft crystal B phase is identified based on the slight change in birefringence and the formation of tiny transition bars across the fan boundary when viewed under the polarising microscope (Figure 4).[46] In the DSC thermograms of second heating (Figure 5), an endotherm attributable to the soft crystal-mesophase transition is observed at 57.8°C. Therefore, this confirms that a transition takes place at lower temperature. In addition, Cladis and Goodby have proposed that the transition of SmA to crystal B is usually marked by the appearance of transient transition bars.[47] The presence of soft crystal B phase in **3b** is further substantiated by the XRD analysis which will be discussed in the following section.

As for compound **3c** which possesses terminal Br atom, it exhibits enantiotropic SmA behaviour upon heating–cooling. Once again, the SmA phase is assigned from the formation of batonnets at the transition which is then coalesced to give a focal-conic fan-shaped texture. In addition, the bromo-substituted star-shaped mesogens also show similar observation as discussed for compound **3b**. The soft crystal transition is verified and further substantiated by the DSC

Table 2. Phase transition temperature (°C) and associated enthalpy changes (kJ mol^{-1}) for star-shaped compounds **3a–3f** upon heating and cooling.

Compound	Phase transition temperatures, °C (ΔH, kJ mol^{-1})
3a (X = F)	Cr_1 99.8 (30.6) Cr_2 110.2 (24.3) I
	I 87.6 (12.2) SmA 73.7 (43.7) Cr
3b (X = Cl)*	Cr B 57.8 (1.2) SmA 110.7 (5.2) N 114.5 (4.5) I
	I 111.2(4.3) N 108.7 (4.8) SmA 55.3 (1.4) Cr B
3c (X = Br)*	Cr B 90.4 (1.6) SmA 132.0 (16.3) I
	I 130.2 (15.8) SmA 88.0 (1.7) Cr B
3d (X = I)	Cr_1 77.5 (6.1) Cr_2 122.2 (38.1) SmA 138.6 (12.8) I
	1120.9 (10.4) SmA 110.2 (31.6) Cr
3e (X = C_2H_5)	Cr_1 95.8 (10.8) Cr_2 105.2 (43.5) I
	I 85.1 (0.5) N 66.7 (33.1) Cr
3f (X = OC_2H_5)	Cr 139.5 (46.8) N 151.3 (3.8) I
	I 148.8 (3.7) N 78.1 (28.8) Cr

Notes: Cr B, soft crystal B phase; Cr, Crystal; SmA, smectic A; N, nematic; I, isotropic.
Phase sequence and temperature upon cooling are shown in italic.
*Phase transition temperatures and enthalpy changes are taken on the second heating–cooling cycle.

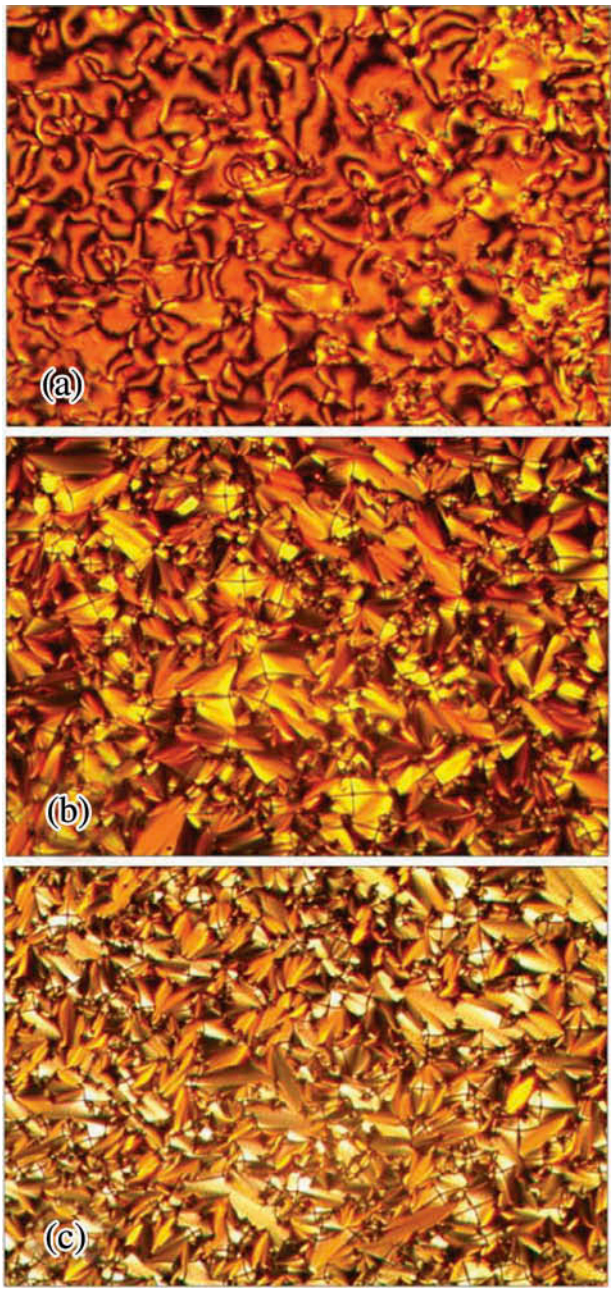

Figure 4. (colour online) Optical photomicrograph of star-shaped mesogens **3b** (X = Cl) exhibiting the (a) Schlieran texture of N phase which eventually transform into the (b) fan-shaped texture of SmA phase. (c) On further cooling, a change in birefringence along with the appearance of small transition bars across the fan of the soft crystal B phase.

thermogram. For instance, **3c** exhibits SmA phase at high temperature and on cooling to room temperature, the fan-shaped optical texture remains unchanged although the sample is subjected to mechanical stress. On careful observation during cooling, there is no indication for this compound getting crystallised even after cooling the sample to room temperature. Instead, slow transformation of fan-shaped texture accompanied by tiny transition bars is observed and this is supported by the DSC thermogram of **3c**, whereby a small transition peak is observed at 88°C. Compounds **3b** and **3c** tend to form soft crystalline state at lower temperature and this can be due to the combined effect of the long flexible alkyl spacer and the rigid aromatic core in the molecular structure, which hindered the crystallisation process of the compound.[48] Compound **3d** shows predominantly enantiotropic smectic behaviour in their liquid-crystalline state whereby the phase sequence of Cr–SmA–Iso is recorded in heating and cooling cycles. Upon heating compound **3d** under polarised light, the crystal phase melts into a viscous fluid at 122°C along with the appearance of focal conic texture characteristic of SmA phase before turning into the isotropic phase at higher temperature. On cooling, the formation of batonnets emanating from the distinct black isotropic region is observed. The tiny batonnets eventually coalesced to give the fan-shaped texture before undergoing crystallisation at 110°C. The POM investigation is also supported by the DSC traces obtained for **3d** whereby the formation of enantiotropic SmA phase is observed upon heating–cooling compound **3d**. On the other hand, the ethyl- and ethoxy-substituted star-shaped mesogens (**3e** and **3f**) show predominant N behaviour. The N phase of both mesogens show a pseudo-isotropic texture, which flashed when subjected to shearing stress. By comparing compounds **3e** and **3f**, **3f** is found to display higher thermal stability as indicated by the higher clearing point (151.3°C). The DSC thermogram of compound **3f** upon heating-cooling cycle is depicted in Figure 6. In addition, **3f** tends to exhibit enantiotropic N phase while **3e** only exhibits monotropic behaviour. As a result, the presence of high-electronegativity oxygen atom in **3f** may exert an effect towards the mesomorphic behaviour of the compound as one would have expected. A similar observation was also reported for the non-conventional azo-based H-shaped symmetrical dimer whereby the methoxy series possess higher mesophase temperature in comparison to the methyl series.[49]

It is also noteworthy to mention that the entropy change associated with the N–isotropic transition for compounds **3b**, **3e** and **3f**, expressed as the dimensionless quantity, $\Delta S_{NI}/R$, are found to be in the range of 0.17–1.35 which is considered lower than those normally observed for LC oligomers.[50,51] As documented, such reduction in entropy can be attributed to the conformations of these molecules in which the biaxiality of the mesogenic groups has been increased. Hence, the enhanced biaxiality has the effect of reducing the entropy change and this behaviour is not unusual as similar finding have been reported

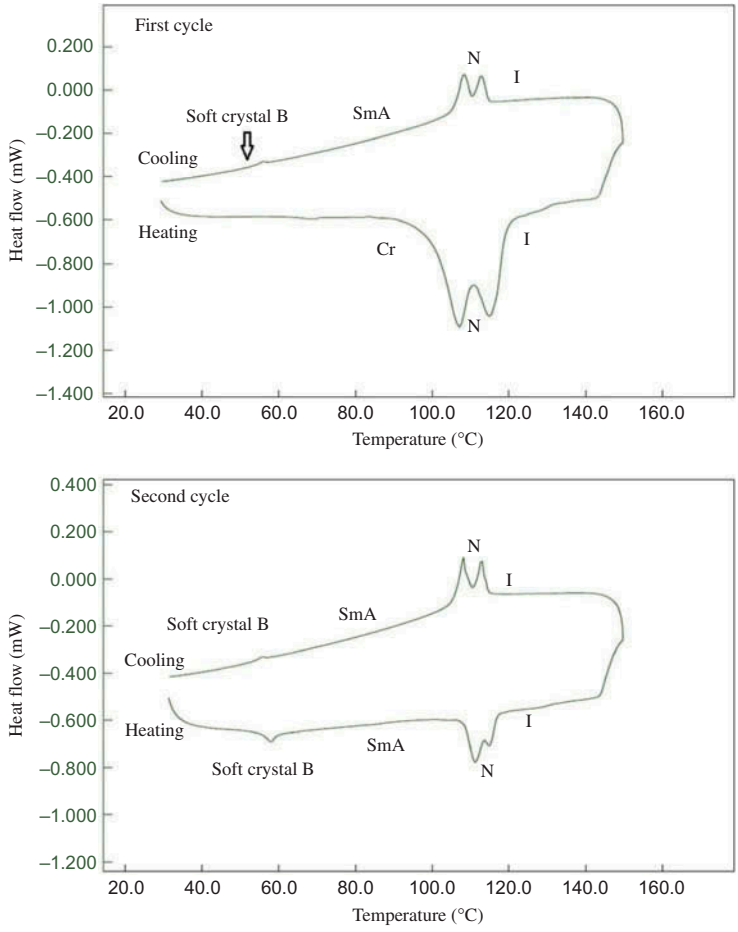

Figure 5. (colour online) DSC thermograms of star-shaped mesogen **3b** (X = Cl) upon heating–cooling run for two cycles at the rate of ±5°C.

previously in other oligomeric compounds whereby the conformations of these compounds is said to be rather biaxial in nature.[52,53]

Overall, the influence of different terminal substituent towards the mesomorphic behaviour can also be regarded as one of the factors contributing to the difference of clearing temperatures. The clearing temperature decreases with respect to the terminal substituent in the following order:

$$OC_2H_5 > I > Br > Cl > F > C_2H_5 \quad (1)$$

Based on the above order, the $–OC_2H_5$ group possesses the highest stability. This can be explained in terms of the lone pairs of oxygen which is shielded by an insulator-like ethyl group. The repulsive forces involving the oxygen lone pair are thereby substantially reduced and allow a close approach of the neighbouring molecules resulting in an increment of bonding forces. Eventually, this leads to an increase in the clearing temperature. The mesophase–isotropic transition temperature of $–C_2H_5$ is less than the halogen atoms because the ethyl group is less polar while halogen atom will provide the molecule with higher polarity, high thermal attraction, and hence higher clearing temperature.[54] Besides, the difference in molecular geometry resulting from the change in bond angle between ethyl- and ethoxy-substituted star-shaped mesogens is accountable for the difference in the transitional behaviour of these mesogens whereby the greater shape anisotropy of the ethoxy-substituted mesogen is expected to give rise to higher mesophase–isotropic transition temperature.[55] Hence, the prediction of this theoretical model developed by Imrie and Luckhurst is in good agreement with the experimental data obtained.[56] If we consider the clearing temperature among the halogen atoms, the order appears to follow a regular trend across the series whereby the fluorine-substituted star-shaped mesogen conferred a lower thermal degree due

to the smallest radius while iodine atom exhibits the highest clearing point. This observation is consistent with the reported trend of α-(4-benzylidene-substituted-aniline-4′-oxy)-ω-[pentyl-4-(4′-phenyl)benzoateoxy]hexane series and can be rationalised in term of the size of the halogen whereby the order of clearing temperature is linearly dependent on the size of the terminal halogen.[57] In addition, it is also worthwhile to mention that similar order of clearing points in relation to the terminal substituents is observed for the intermediate substituted-azobenzene **2a**–**2d** possessing merely halogen atoms.

3.2 *Comparative study between compounds 3a–3f and previously reported 4a–4e*

The present star-shaped compounds **3a–3f** are selected for comparison purpose with the previously documented star-shaped mesogens 1,3,4-tris{(4-benzylidene-substituted-aniline-4-oxy)hexyloxy}benzene (**4a–4e**) [42] and the general molecular structure is shown below.

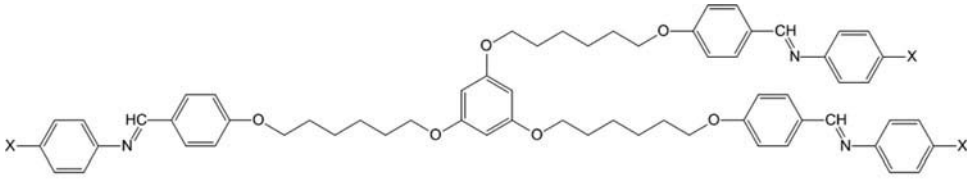

Compound	X
4a	F
4b	Cl
4c	Br
4d	I
4e	C_2H_5

By comparing the mesomorphic properties between the present symmetrical star-shaped compounds with the previously reported Schiff base analogous compounds, one significant similarity is that both series exhibit calamitic mesophases. For instance, compounds of present series show N and SmA phases while compounds of series **4** exhibit N, SmA as well as SmC phases. Moreover, both linkages behave in a similar fashion whereby they are found to be very favourable to mesomorphism which can be resulted from the rigidity of the molecule given by the double bond.

However, the advantage of liquid-crystalline azobenzene compounds over the Schiff base counterparts is that they are thermally more stable than the Schiff base star-shaped mesogens. For instance, the clearing temperature for **4c** (X = Br) is 108.1°C, but for the present azo mesogen **3c** (X = Br), the clearing point is higher (132.0°C). In addition, the presence of azo linkage in liquid-crystalline compounds also makes them suitable for physical studies especially in determining the photo-induced effect. The difference observed between the two series is that the title compound **3e** (X = C_2H_5) shows solely monotropic N behaviour but for **4e** (X = C_2H_5) it exhibits monotropic N and SmA phases upon cooling. Hence, the absence of smectic phase in the star-shaped mesogen **3e** can be ascribed to the variation of dipole moment between the azo linkage (–N=N–) which has zero dipole moment while the azomethine linkage (–CH=N–) possesses higher polarity due to the presence of the effective charge between C and N atom.[58] As a result, the greater dipole moment eventually increases the molecular polarisability and intermolecular cohesive forces leading to the smectic properties in compound **4e**. Furthermore, the imine –CH=N– possesses greater tendency to induce smectic mesomorphism in comparison to the–N=N– linkage.[59] This phenomenon is broadly consistent with those observed for conventional low-molar mass liquid crystals possessing azomethine linking group.[58,60,61]

3.3 *XRD analysis*

XRD study has been carried out on a representative compound **3b** (X = Cl) in order to provide more detailed information on the liquid-crystalline phase structures of the star-shaped mesogen. From the XRD data of **3b**, the presence of N phase is confirmed based on the XRD pattern at 110°C (Figure 7), whereby no peak is recorded at small angle but a broad peak at the wide-angle region 2θ = 17.04° (with *d*-spacing value of 0.45 nm) is observed in the XRD diffractogram, thus indicating a liquid-like order of N phase. Figure 8 shows the

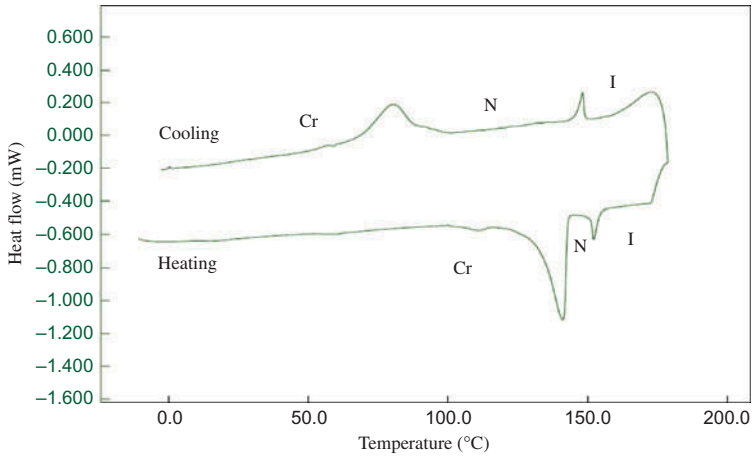

Figure 6. (colour online) DSC thermograms of star-shaped mesogen **3f** (X = OC_2H_5) upon heating–cooling run at the rate of ±5°C.

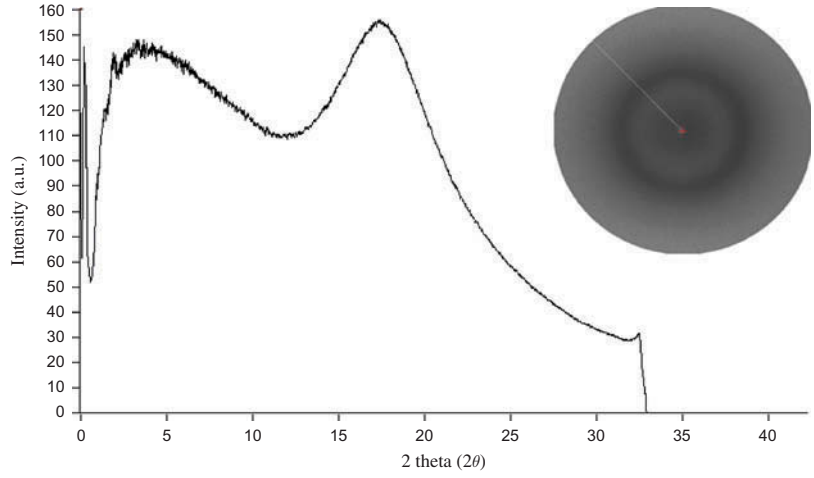

Figure 7. (colour online) The intensity versus 2θ profile for the X-ray diffraction pattern of compound **3b** at 110°C during the cooling process.

intensity versus 2θ profile for the XRD powder pattern of the SmA phase exhibited by **3b**. At 70°C, an obvious sharp peak is evident in the low angle 2θ = 3.286° (with the *d*-spacing value of 2.326 nm) which could verify the presence of lamellar structure (smectic-layered arrangement) of the SmA phase in **3b**. A broad peak associated with the lateral packing at 2θ = 17.91° (with the *d*-spacing value of 0.428 nm) can be observed in wide-angle XRD curve. In the wide-angle region a diffuse reflection is seen with a spacing of 0.428 nm corresponding to the intermolecular separation within the smectic layer due to the liquid-like positional correlation.[62] At lower temperature, **3b** is said to exhibit soft crystal B phase. From the XRD spectrum of **3b** taken at 50°C (Figure 9), a sharp peak has been detected at 2θ = 18.17° (with the *d*-spacing value of 0.422 nm) as a confirmation of this phase. Overall, the XRD date of **3b** is summarised in Table 3.

According to the molecular modelling, chain length of 2.27 nm in the branched arms of compound **3b** (X = Cl) and its *d*-spacing value of 2.33 nm in the smectic phase, a possible molecular arrangement in the smectic layer of **3b** is shown in Figure 10, whereby the lateral distance of branched arms *l* = 0.43 nm corresponding to 2θ = 17.91°. It is assumed that the peripheral rod-like units are organised in a common layer together with the disc-like benzene core. Compound **3c** (X = Br) is found to exhibit SmA phase and by comparing this two homologues, due to the smaller size of the chlorine atom with a less steric hindrance, **3b** has a shorter intermolecular distance to induce a stronger layer interaction in the smectic phase in comparison to **3c**.

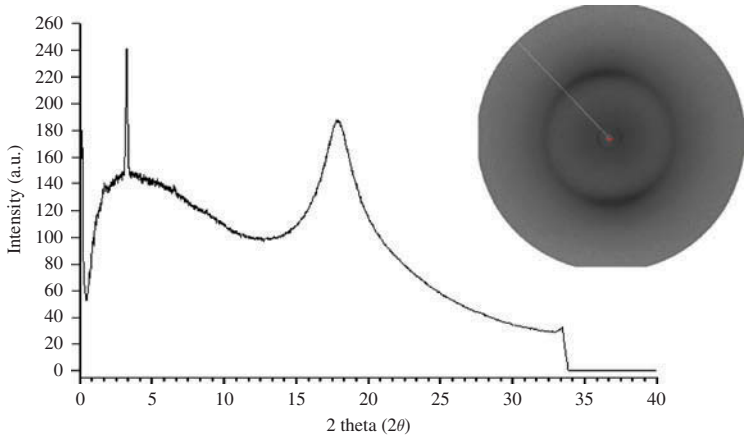

Figure 8. (colour online) The intensity versus 2θ profile for the X-ray diffraction pattern of compound **3b** at 70°C during the cooling process.

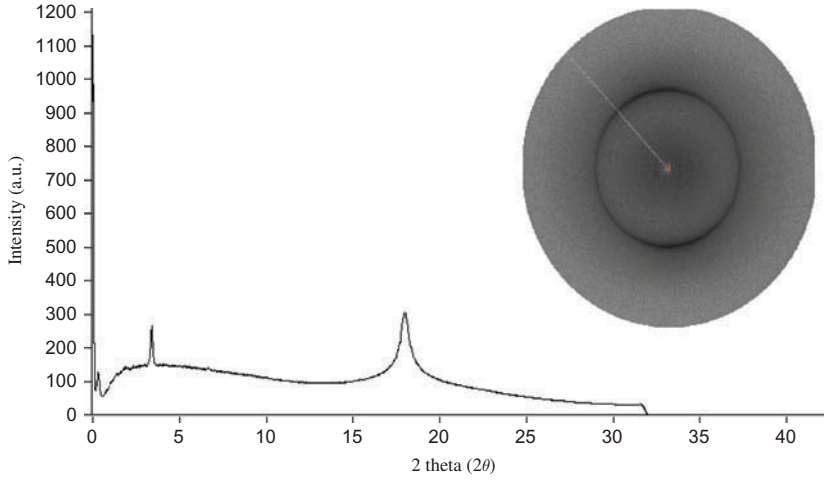

Figure 9. (colour online) The intensity versus 2θ profile for the X-ray diffraction pattern of compound **3b** at 50°C during the cooling process.

The generation of smectic arrangement by the trimeric star-shaped mesogens can be attributed to the side-by-side organisation of the azobenzene peripheral units which lie parallel to each other. This kind of possible molecular arrangement as proposed in Figure 10 explains why only the calamitic N or smectic phase is present instead of a discotic columnar phase because the introduction of the hexylene spacer between the benzene core and azobenzene peripheral units is flexible enough to allow the peripherals to rotate freely. As a result, the rod-like peripheral units can align parallel to each other which favour the side-by-side interaction with neighbouring molecules and not the molecular stacking structure as seen in the discotic phase.

Table 3. XRD data (2θ and *d*-spacing values) of the selected liquid crystalline compound **3b** (X = Cl) upon cooling.

Compound	Temperature (°C)	2θ (°)		*d*-spacing (nm)	
3b (X = Cl)	110	–	17.04	–	0.45
	100	3.174	17.47	2.408	0.439
	90	3.263	17.62	2.342	0.435
	70	3.286	17.91	2.326	0.428
	50	3.378	18.17	2.262	0.422

Note: – means no peak

In summary, the formation of smectic order is governed by the rod-like azobenzene while the benzene core acts only as a linking group interconnecting the rods. This type of possible conformation adopted by the title mesogens in the smectic phase can also be rationalised by the earlier statement used to justify the

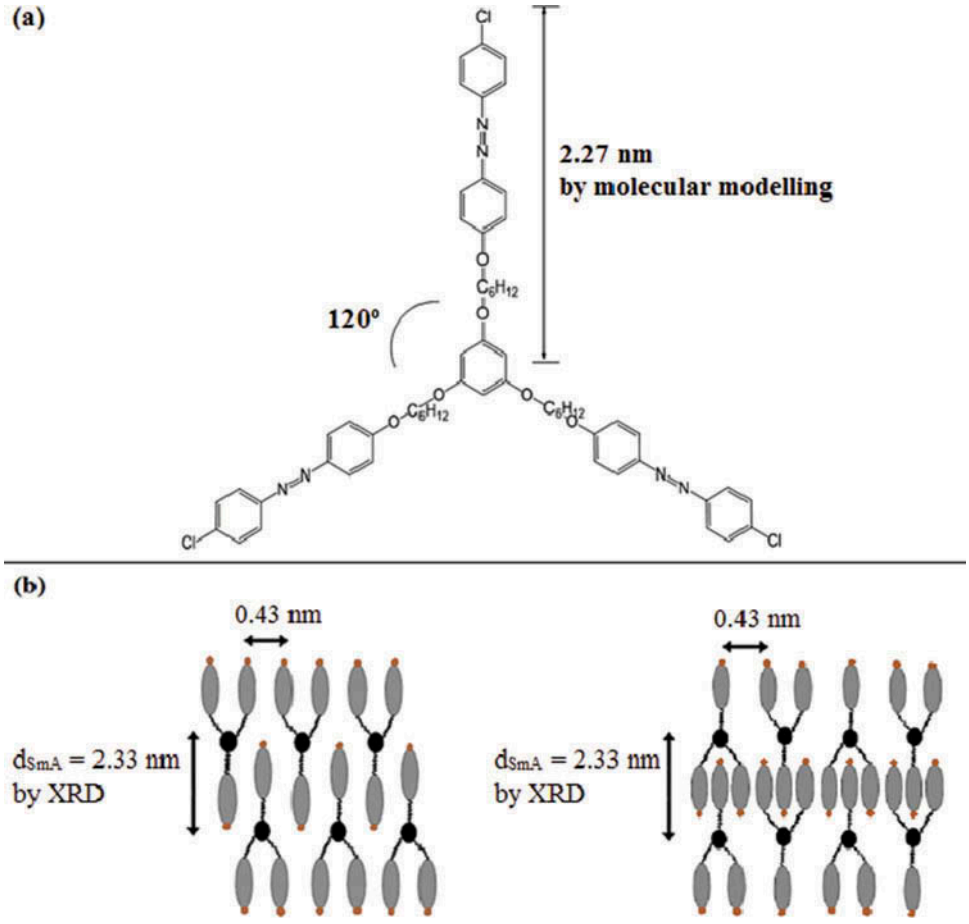

Figure 10. (colour online) Schematic diagrams of molecular arrangements for compound **3b**: (a) molecular modelling of the branched arm length, (b) sketch of the possible molecular packing of **3b** in the smectic phase.

molecular packing system of smectic phase formed by the non-conventional three-armed star-shaped mesogens.[35,63] Furthermore, the proposed smectic arrangement is also in accord with the recent reported three-armed star-shaped mesogens based on benzene 1,3,5-tricarboxylic acid.[64]

3.4 Photosensitivity studies

The preliminary studies of the photochemical properties were carried out on compounds **3a–3f** as the compounds consist of azo –N=N– linkage. In order to obtain the UV–Visible spectra, chloroform ($CHCl_3$) was used as the solvent to dissolve the samples. The UV–Visible absorption spectra of all star-shaped mesogens are depicted in Figure 11 and the absorption maximums are summarised in Table 4. All the absorption spectra are almost identical for the six compounds due to the same molecular structure, with variation in the terminal substituent (X). However, a clear trend can be observed in the absorption spectra involving the halogenated compounds **3a–3d**. The high-intensity absorption peak at 350–360 nm is related to the π–π* electronic transition of the chromophores. The occurrence of photoisomerisation can be induced with the aid of UV–Vis absorption spectra of the sample in the absence and upon illumination with UV light. As a representative, compound **3f** is introduced for photoisomerisation studies. Figure 12 shows the UV spectra of **3f** obtained at different conditions. The UV spectrum of a freshly prepared solution is labelled as 12(a). Since the peak at 240 nm is corresponded to the solvent cut-off wavelength by the chloroform, thus discussion of this peak will not be described. In the absence of UV irradiation, the absorption peak appears at 359 nm can be related to the absorption of *trans* form of –N=N– linkage. Subsequently, the solution was irradiated using UV light with a wavelength of 365 nm for 15 min in order to induce *trans–cis* isomerisation. The UV–Vis spectrum thus recorded is depicted in Figure 12(b). The peak at 450 nm (n-π*) starts to appear which can be attributed to the absorption of *cis* form of –N=N– linkage. Further irradiation with UV light on **3f** for

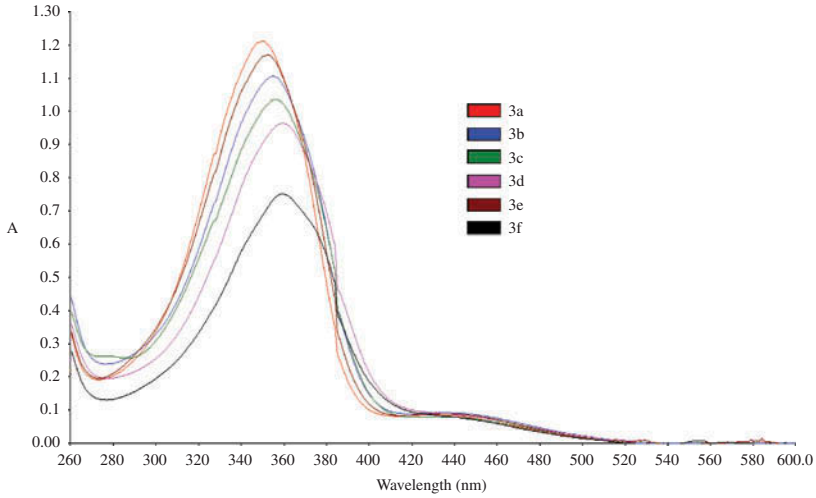

Figure 11. (colour online) UV–Visible absorption spectra of star-shaped mesogens **3a–3f** in chloroform.

Table 4. UV–Visible results of the star-shaped compounds **3a–3f**.

	Absorbance, nm	
Compound	λ_{max}	λ_{max}
3a (X = F)	246	350
3b (X = Cl)	247	355
3c (X = Br)	247	356
3d (X = I)	247	359
3e (X = C_2H_5)	246	353
3f (X = OC_2H_5)	247	359

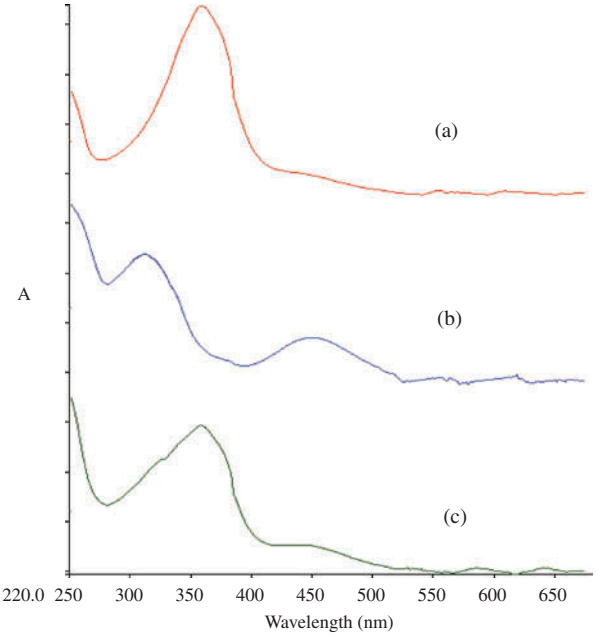

Figure 12. (colour online) UV–Visible absorption spectra of compound 3f in chloroform. (a) Fresh solution (b) after exposure (15 min) to 365 nm UV light (c) after keeping the exposed solution in the dark, overnight.

another 15 min produces the same UV–Vis spectrum as shown in Figure 12(b). Hence, this indicates that the optimum photostationary state is reached. As noted in literature, return of *trans* form can take place either by shining white light of wavelength 400–500 nm, or by keeping the solution in the dark.[65] The respective solution was kept in the dark for 24 h and once again the UV–Vis spectrum was recorded Figure 12(c). After the solution being left in the dark, the peak at 450 nm almost disappears owing to the *cis* to *trans* isomerisation of –N=N– linkage. Therefore, the star-shaped molecule is capable to show photoisomerisation behaviour in solution. The recovery of reverting back to the *trans* form from the photo-excited *cis* form has occurred but this back-relaxation process is found to be very slow.

Based on Table 4, as the fluorine at *para*-postition of the azobenzene ring was substituted by iodine, a gradual shift of the λ_{max} towards a longer wavelength region is observed. This can be attributed to the reduced electronegativity order of the halogen substituent and their conjugation effect with the π-electrons of the aromatic ring. Hence, the substitution of different halogen at the *para*-position can influence the UV-absorption band and result in a bathochromic shift (a shift to a longer wavelength) when changing from strong electron-withdrawing fluorine to weak electron-withdrawing iodine atom.[66] For instance, **3a** (X = F) displays the lowest λ_{max} (350 nm) while **3d** shows the highest value of λ_{max} (359 nm). This trend is also consistent with those UV spectra observed for compounds 5-substituted-4-thio-2′-deoxyuridine

nucleosides possessing various lateral substituents X = H, CH_3, F, Cl, Br, I.[67]

4. Conclusion

A series of six new symmetrical three-armed star-shaped compounds comprising three terminal substituted-azobenzene fragment units with phloroglucinol as central core, namely 1,3,5-tris-{4-[(4-substituted-phenyl)diazenyl]phenoxy}-6′-hexyloxy benzene, **3a–3f** have been synthesised and characterised. All the star-shaped compounds showed liquid-crystalline properties whereby N and SmA phases were observed. Interestingly, on cooling compounds **3b** and **3c** transformed into a soft crystalline state accompanied with small enthalpy change. The thermal stabilities of the star-shaped mesogens were relatively higher as compared to those of the earlier-reported analogous star-shaped mesogens. Hence, the mesophases of the title compounds were stabilised over a wide thermal range. In addition, the POM studies along with the XRD result confirm the formation of N and smectic phases in the star-shaped mesogen possessing chloro terminal substituent and a possible molecular arrangement of this compound in SmA phase is proposed. Overall, the experimental results have substantiated that the peripheral azobenzene fragments influence the phase behaviour and thermal stability of the mesogens while the benzene core unit serves as a linking group, interconnecting the rod-like peripheral units. As the terminal substituent (X) is varied, the clearing point and mesomorphic properties of the star-shaped mesogen differ.

Acknowledgement

Y.-H. Ooi would like to acknowledge the Ministry of Higher Education of Malaysia (MOHE) for the research assistantship under the scheme MyBrain15.

Funding

The main author (G.-Y. Yeap) would like to thank Universiti Sains Malaysia (USM) for the funding of research [grant no. 203/PKIMIA/6711265] and the laboratory facilities.

References

[1] Yoshizawa A. Unconventional liquid crystal oligomers with a hierarchical structure. J Mater Chem. 2008;18:2877–2889. doi:10.1039/b802712a

[2] Achalkumar AS, Hiremath US, Shankar Rao DS, Yelamaggad CV. Non-conventional liquid crystals: synthesis and mesomorphism of non-symmetric trimers and tetramers derived from cholesterol. Liq Cryst. 2011;38:1563–1589. doi:10.1080/02678292.2011.610473

[3] Gemming S, Popov I, Lehmann M. Polymorphism in liquid crystals from star-shaped mesogens. Phil Mag Lett. 2007;87:883–891. doi:10.1080/09500830701537959

[4] Yao DS, Zhang BY, Li YH, Xiao WQ. Synthesis and mesomorphism of novel star-shaped glassy liquid crystals containing pentaerythritol esters. Tetrahedron Lett. 2004;45:8953–8956. doi:10.1016/j.tetlet.2004.09.109

[5] Tian M, Zhang BY, Cong YH, Zhang N, Yao DS. Mesomorphic properties of multi-arm liquid crystals containing glucose and sorbitol as cores. J Mol Struct. 2009;923:39–44. doi:10.1016/j.molstruc.2009.01.049

[6] Shimizu Y, Kurobe A, Monobe H, Terasawa N, Kiyohara K, Uchida K. Calamitic and discotic mesophases formed by kinetically controlled rod-disc alternation of molecular shape in a triphenylene-azobenzene mesogenic system. Chem Comm. 2003;14:1676–1677. doi:10.1039/b301862h

[7] Takezoe H, Takanishi Y. Bent-core liquid crystals: their mysterious and attractive world. Jap J App Phys. 2006;45:597–625. doi:10.1143/JJAP.45.597

[8] Balamurugan S, Kannan P. Synthesis and characterization of symmetrical banana shaped liquid crystalline polyethers. J Mol Struct. 2009;934:44–52. doi:10.1016/j.molstruc.2009.06.019

[9] Wang H, Zheng Z, Shen D. Blue phase liquid crystals induced by bent-shaped molecules based on 1,3,4-oxadiazole derivatives. Liq Cryst. 2012;39:99–103. doi:10.1080/02678292.2011.628704

[10] Dingemans TJ, Madsen LA, Francescangeli O, Vita F, Photinos DJ, Poon CD, Samulski ET. The biaxial nematic phase of oxadiazole biphenol mesogens. Liq Cryst. 2013;40:1655–1677. doi:10.1080/02678292.2013.824119

[11] Lee HC, Lu Z, Henderson PA, Achard MF, Mahmood WAK, Yeap GY, Imrie CT. Cholesteryl-based liquid crystal dimers containing a sulfur-sulfur link in the flexible spacer. Liq Cryst. 2012;39:259–268. doi:10.1080/02678292.2011.641753

[12] Mori A, Kubo K, Takemoto M, Kitaura H, Ujiie S. Dimeric liquid crystals with 5-(4-alkoxybenzoyloxy) tropone or 4-(4-alkoxybenzoyloxy)phenyl cores: evaluation of the tilt angles of the cores, spacers, and side chains. Liq Cryst. 2006;33:521–530. doi:10.1080/02678290600633253

[13] Yeap GY, Al-Taifi EA, Ong CH, Mahmood WAK, Takeuchi D, Ito MM. Synthesis and phase transition studies on non-symmetric liquid crystal dimers: N-(4-(n-(4-(benzothiazol-2-yl)phenoxy)alkyloxy)-benzylidene)-4-chloroanilines. Phase Trans. 2012;85:483–496. doi:10.1080/01411594.2011.624278

[14] Henderson PA, Imrie CT. Methylene-linked liquid crystal dimers and the twist-bend nematic phase. Liq Cryst. 2011;38:1407–1414. doi:10.1080/02678292.2011.624368

[15] Buzin AI, Makarova NN, Taldrik AV, Malakhova YN, Bushmarinov IS, Antipin MY. Comb-shaped liquid crystalline stereoregular cyclolinear methylsiloxane copolymers: synthesis, behaviour in bulk and behaviour in monolayers. Liq Cryst. 2012;39:133–147. doi:10.1080/02678292.2011.620989

[16] Jung BM, Huang YD, Chang JY. Preparation of discotic metallomesogens based on phenacylpyridines

showing room temperature columnar phases. Liq Cryst. 2010;37:85–92. doi:10.1080/02678290903390940

[17] Rezvani Z, Divband B, Abbasi AR, Nejati K. Liquid crystalline properties of copper(II) complexes derived from azo-containing salicylaldimine ligands. Polyhedron. 2006;25:1915–1920. doi:10.1016/j.poly.2005.12.016

[18] Abe Y, Nakazima N, Tanase T, Katano S, Mukai H, Ohta K. Syntheses, structures, and mesomorphism of a series of Cu(II) salen complexes with 4-substituted long alkoxy chains. Mol Cryst Liq Cryst. 2007;466:129–147. doi:10.1080/15421400601150304

[19] Lee JH, Han MJ, Hwang SH, Jang I, Lee SJ, Yoo SH, Jho JY, Park SY. Self-assembled discotic liquid crystals formed by hydrogen bonding of alkoxystilbazoles. Tetrahedron Lett. 2005;46:7143–7146. doi:10.1016/j.tetlet.2005.08.094

[20] Goldmann D, Janietz D, Schmidt C, Wendorff JH. Columnar liquid crystalline phases through hydrogen bonding and nanoscale segregation. J Mater Chem. 2004;14:1521–1525. doi:10.1039/b400781f

[21] Cho CM, Wang X, Li JJ, He C, Xu J. Synthesis and self-assembly of halogen-bond donor-spacer-hydrogen-bond donor molecules: polymeric liquid crystals induced by combination of intermolecular halogen- and hydrogen-bonding interactions. Liq Cryst. 2013;40:185–196. doi:10.1080/02678292.2012.735708

[22] Martinez-Felipe A, Lu Z, Henderson PA, Picken SJ, Norder B, Imrie CT, Ribes-Greus A. Synthesis and characterisation of side chain liquid crystal copolymers containing sulfonic acid groups. Polymer. 2012;53:2604–2612. doi:10.1016/j.polymer.2012.02.029

[23] Hashim R, Sugimura A, Minamikawa H, Heidelberg T. Nature-likesynthetic alkyl branched-chain glycolipids: a review on chemical structure and self-assembly properties. Liq Cryst. 2012;39:1–17. doi:10.1080/02678292.2011.614017

[24] Cook AG, Martinez-Felipe A, Brooks NJ, Seddon JM, Imrie CT. New insights into the transitional behaviour of methyl-6-O-(n-dodecanoyl)-α-D-glucopyranoside using variable temperature FTIR spectroscopy and X-ray diffraction. Liq Cryst. 2013;40:1817–1827. doi:10.1080/02678292.2013.854556

[25] Lee JH, Jang I, Hwang SH, Lee SJ, Yoo SH, Jho JY. Self-assembled discotic nematic liquid crystals formed by simple hydrogen bonding between phenol and pyridine moieties. Liq Cryst. 2012;39:973–981. doi:10.1080/02678292.2012.689020

[26] Lee JH, Lee HJ, Lee SJ, Jang J, Yoo SH, Jho JY. Preparation of conjugated polymeric columns with a hexagonal symmetry from star-shaped supramolecular liquid crystals. Liq Cryst. 2013;40:112–119. doi:10.1080/02678292.2012.733737

[27] Imrie CT, Henderson PA, Yeap GY. Liquid crystal oligomers: going beyond dimers. Liq Cryst. 2009;36:755–777. doi:10.1080/02678290903157455

[28] Lehmann M. Star mesogens (Hekates) – Tailor made molecules for programming supramolecular functionality. Chem Eur J. 2009;15:3638–3651. doi:10.1002/chem.200802625

[29] Jeong KU, Jing AJ, Monsdorf B, Graham MJ, Harris FW, Cheng SZD. Self-assembly of chemically linked rod−disc mesogenic liquid crystals. J Phys Chem B. 2007;111:767–777. doi:10.1021/jp066274b

[30] Imrie CT, Lu Z, Picken SJ, Yildirim Z. Oligomeric rod-disc nematic liquid crystals. Chem Comm. 2007;1245–1247. doi:10.1039/b614922g

[31] Lehmann M, Gearba RI, Ivanov DA, Koch MHJ. New star-shaped mesogens with three different arms on a 1,3,5-benzene core. Mol Cryst Liq Cryst. 2004;411:397–406. doi:10.1080/15421400490435422

[32] Meier H, Lehmann M, Holst HC, Schwöppe D. Star-shaped conjugated compounds forming nematic discotic systems. Tetrahedron. 2004;60:6881–6888. doi:10.1016/j.tet.2004.06.012

[33] Stackhouse PJ, Wilson A, Lacey D, Hird M. Synthesis and properties of novel columnar liquid crystals based on symmetrical and non-symmetrical 1,3,5-trisubstituted benzene derivatives. Liq Cryst. 2010;37:1191–1203. doi:10.1080/02678292.2010.490647

[34] Zhang BY, Yao DS, Meng FB, Li YH. Structure and properties of novel three-armed star-shaped liquid crystals. J Mol Struct. 2005;741:135–140. doi:10.1016/j.molstruc.2005.01.057

[35] Goldmann D, Janietz D, Schmidt C, Wendorff JH. Liquid crystalline 1,3,5-triazines incorporating rod-like azobenzene sub-units. Liq Cryst. 1998;25:711–719. doi:10.1080/026782998205723

[36] Salisu AA, Kogo AA. New Liquid crystals in the series of 1,3,5-triazine compounds containing azobenzene at the peripheral arms. Bayero J Pure and Appl Sci. 2010;3:54–58.

[37] Yao DS, Zhang BY, Zhang WW, Tian M. A new class of star-shaped cholesteric liquid crystal containing a 1,3,5-trihydroxybenzene unit as a core. J Mol Struct. 2008;881:83–89. doi:10.1016/j.molstruc.2007.08.041

[38] Prasad V. Liquid crystalline compounds with V-shaped molecular structures: synthesis and characterization of new azo compounds. Liq Cryst. 2001;28:145–150. doi:10.1080/026782901462481

[39] Yeap GY, Balamurugan S, Rakesh S. Synthesis and mesomorphic properties of chiral liquid crystal dimers derived from azobenzene and substituted naphthol. Liq Cryst. 2013;40:555–563. doi:10.1080/02678292.2013.765608

[40] Bobrovsky A, Shibaev V. Polarised light-induced orientation and reorientation processes and unexpected 'memory effect' in side-chain azobenzene-containing LC polymers. Liq Cryst. 2012;39:339–345. doi:10.1080/02678292.2011.648665

[41] Chan TN, Lu Z, Yam WS, Yeap GY, Imrie CT. Non-symmetric liquid crystal dimers containing an isoflavone moiety. Liq Cryst. 2012;39:393–402. doi:10.1080/02678292.2012.658712

[42] Yeap GY, Ooi YH, Kenji K, Ito MM. Synthesis and mesomorphic properties of novel three-armed star-shaped mesogens of phloroglucinol (1,3,5-trihydroxybenzene) containing Schiff base moiety. Phase Trans. 2013;86:365–379. doi:10.1080/01411594.2012.683870

[43] Al-Hamdani UJ, Gassim TE, Radhy HH. Synthesis and characterization of azo compounds and study of the effect of substituents on their liquid crystalline behavior. Molecules. 2010;15:5620–5628. doi:10.3390/molecules15085620

[44] Attard GS, Dave JS, Wallington A, Imrie CT, Karasz FE. Transitional properties of liquid-crystalline side-chain polymers derived from poly(p-hydroxystyrene. Makromol Chem. 1991;192:1495–1508. doi:10.1002/macp.1991.021920704

[45] Ha ST, Ng MY, Subramaniam RT, Ito MM, Saito A, Watanabe M, Lee SL, Bonde NL. Mesogenic azomethine esters with different end groups: Synthesis and thermotropic properties. Int J Phy Sci. 2010;5:1256–1262.
[46] Dierking I. Textures of liquid crystals. Weinheim: Wiley-VCH; 2003. p. 141–142.
[47] Cladis PE, Goodby JW. Pressure study of a hexatic B and crystal B phase. Mol Cryst Liq Cryst. 1982;72:307–312. doi:10.1080/01406568208084725
[48] Bao R, Pan M, Qiu JJ, Liu CM. Synthesis and characterization of six-arm star-shaped liquid crystalline cyclotriphosphazenes. Chin Chem Lett. 2010;21:682–685. doi:10.1016/j.cclet.2009.12.020
[49] Prajapati AK, Varia MC, Sahoo SP. Azoester-based H-shaped symmetrical mesogenic dimers containing –CH3/-OCH3 terminal substituent. Phase Trans. 2011;84:325–342. doi:10.1080/01411594.2010.537210
[50] Henderson PA, Imrie CT. Semiflexible liquid crystalline tetramers as models of structurally analogous copolymers. Macromolecules. 2005;38:3307–3311. doi:10.1021/ma0502304
[51] Imrie CT, Luckhurst GR. Liquid crystal trimers. The synthesis and characterisation of the4,4′-bis[ω-(4-cyanobiphenyl-4′-yloxy)alkoxy]biphenyls. J Mater Chem. 1998;8:1339–1343. doi:10.1039/a801128a
[52] Yeap GY, Hng TC, Yeap SY, Gorecka E, Ito MM, Ueno K, Okamoto M, Mahmood WAK, Imrie CT. Why do non-symmetric dimers intercalate? The synthesis and characterisation of the α-(4-benzylidene-substituted-aniline-4′-oxy)-ω-(2-methylbutyl-4′-(4″-phenyl) benzoateoxy)alkanes. Liq Cryst. 2009;36:1431–1441. doi:10.1080/02678290903271504
[53] Donaldson T, Henderson PA, Achard MF, Imrie CT. Non-symmetric chiral liquid crystal trimers. Liq Cryst. 2011;38:1331–1339. doi:10.1080/02678292.2011.613265
[54] Thaker BT, Kanojiya JB, Tandel RS. Effects of different terminal substituents on the mesomorphic behavior of some Azo-Schiff base and Azo-Ester-based liquid crystals. Mol Cryst Liq Cryst. 2010;528:120–137. doi:10.1080/15421406.2010.504632
[55] Henderson PA, Niemeyer O, Imrie CT. Methylene-linked liquid crystal dimers. Liq Cryst. 2001;28:463–472. doi:10.1080/02678290010007558
[56] Imrie CT, Luckhurst GR. Liquid crystal dimers and oligomers. In: Demus D, Goodby JW, Gray GW, Spiess HW, Vill V, editors. Handbook of liquid crystals, Vol. 2B. Weinheim: Wiley-VCH; 1998. p. 801.
[57] Yeap GY, Lee HC, Mahmood WAK, Imrie CT, Takeuchi D, Osakada K. Synthesis, thermal and optical behaviour of non-symmetric liquid crystal dimers α-(4-benzylidene-substituted-aniline-4′-oxy)-ω-[pentyl-4-(4′-phenyl)benzoateoxy]hexane. Phase Trans. 2011;84:29–37. doi:10.1080/01411594.2010.513613
[58] Yeap GY, Alshargabi A, Ito MM, Mahmood WAK, Takeuchi D. Synthesis and anisotropic properties of azo-bridged benzothiazole-phenyl esters. Mol Cryst Liq Cryst. 2012;557:126–133. doi:10.1080/15421406.2011.637744
[59] Tinh NH, Zann A, Dubois JC. Synthesis of 1-(4-alkoxy or alkyl-benzoyloxy-phenyl)-2-(4′-pentylphenyl)-ethanes. Influence of the central group on the mesomorphic properties. Mol Cryst Liq Cryst. 1979;53:43–54. doi:10.1080/00268947908083982
[60] Godzwon J, Sienkowska MJ, Galewski Z. Smectic polymorphism of 4-nonyloxybenzylidene-4′-alkyloxyanilines. J Mol Struct. 2007;844–845:259–267. doi:10.1016/j.molstruc.2007.04.029
[61] Yeap GY, Ooi YH, Kubo K, Ito MM. Synthesis and mesomorphic properties of 4-(4-bromopropyloxy)-4′-(4-alkyloxybenzylidene)anilines. Chin Chem Lett. 2012;23:769–772. doi:10.1016/j.cclet.2012.05.008
[62] Yelamaggad CV, Shashikala IS, Hiremath US, Shankar Rao DS, Prasad SK. Liquid crystal dimers possessing chiral rod-like anisometric segments: synthesis, characterization and electro-optic behaviour. Liq Cryst. 2007;34:153–167. doi:10.1080/02678290601137585
[63] Attard GS, Douglass AG, Imrie CT, Taylor L. Liquid crystalline cyclic trimers derived from benzene-1,3,5-tricarboxylic acid. Liq Cryst. 1992;11:779–784. doi:10.1080/02678299208029029
[64] Shanavas A, Narasimhaswamy T, Sadiku ER. Three armed star mesogens based on 1,3,5-benzenetricarboxylic acid: synthesis and mesophase characterization. J Mol Struct. 2013;1054–1055:18–24. doi:10.1016/j.molstruc.2013.09.030
[65] Rahman L, Kumar S, Tschierske C, Israel G, Ster D, Hegde G. Synthesis and photoswitching properties of bent-shaped liquid crystals containing azobenzene monomers. Liq Cryst. 2009;36:397–407. doi:10.1080/02678290902923428
[66] Kang IN, Hwang DH, Shim HK. Synthesis and electrical properties of halogen substituted PPV derivatives. Synthetic Metals. 1995;69:547–548. doi:10.1016/0379-6779(94)02562-D
[67] Zhang X, Xu YZ. NMR and UV Studies of 4-thio-2′-deoxyuridine and its derivatives. Molecules. 2011;16:5655–5664. doi:10.3390/molecules16075655